Chapter 10

Qualitative dynamics, for pedestrians

> The classification of the constituents of a chaos, nothing less is here essayed.
> —Herman Melville, *Moby Dick*, chapter 32

I N THIS CHAPTER we begin to learn how to use qualitative properties of a flow in order to *partition* the state space in a topologically invariant way, and *name* topologically distinct orbits. This will enable us – in chapter 13 – to *count* the distinct orbits, and in the process touch upon all the main themes of this book, going the whole distance from diagnosing chaotic dynamics to computing zeta functions.

We start by a simple physical example, symbolic dynamics of a 3-disk game of pinball, and then show that also for smooth flows the qualitative dynamics of stretching and folding flows enables us to partition the state space and assign symbolic dynamics itineraries to trajectories. Here we illustrate the method on a $1 - d$ approximation to Rössler flow. In chapter 13 we turn this topological dynamics into a multiplicative operation on the state space partitions by means of transition matrices/Markov graphs, the simplest examples of evolution operators. Deceptively simple, this subject can get very difficult very quickly, so in this chapter we do the first pass, at a pedestrian level, postponing the discussion of higher-dimensional, cyclist level issues to chapter 11.

Even though by inclination you might only care about the serious stuff, like Rydberg atoms or mesoscopic devices, and resent wasting time on things formal, this chapter and chapter 13 are good for you. Read them.

10.1   Qualitative dynamics
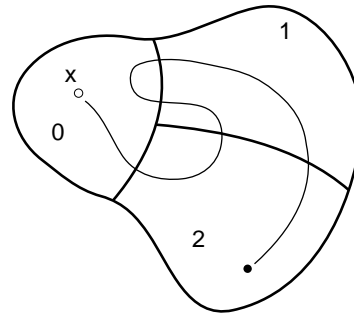
(R. Mainieri and P. Cvitanović)

Figure 10.1: A trajectory with itinerary 021012.

What can a flow do to the state space points? This is a very difficult question to answer because we have assumed very little about the evolution function f^t; continuity, and differentiability a sufficient number of times. Trying to make sense of this question is one of the basic concerns in the study of dynamical systems. One of the first answers was inspired by the motion of the planets: they appear to repeat their motion through the firmament. Motivated by this observation, the first attempts to describe dynamical systems were to think of them as periodic.

However, periodicity is almost never quite exact. What one tends to observe is *recurrence*. A recurrence of a point x_0 of a dynamical system is a return of that point to a neighborhood of where it started. How close the point x_0 must return is up to us: we can choose a volume of any size and shape, and call it the neighborhood $\mathcal{M}_0$, as long as it encloses x_0. For chaotic dynamical systems, the evolution might bring the point back to the starting neighborhood infinitely often. That is, the set

$$\left\{ y \in \mathcal{M}_0 : \quad y = f^t(x_0), \quad t > t_0 \right\} \tag{10.1}$$

will in general have an infinity of recurrent episodes.

To observe a recurrence we must look at neighborhoods of points. This suggests another way of describing how points move in state space, which turns out to be the important first step on the way to a theory of dynamical systems: qualitative, topological dynamics, or, as it is usually called, *symbolic dynamics*. As the subject can get quite technical, a summary of the basic notions and definitions of symbolic dynamics is relegated to sect. 10.5; check that section whenever you run into obscure symbolic dynamics jargon.

We start by cutting up the state space up into regions $\mathcal{M}_A, \mathcal{M}_B, \ldots, \mathcal{M}_Z$. This can be done in many ways, not all equally clever. Any such division of the state space into topologically distinct regions is a *partition*, and we associate with each region (sometimes referred to as a *state*) a symbol s from an N-letter *alphabet* or *state set* $\mathcal{A} = \{A, B, C, \cdots, Z\}$. As the dynamics moves the point through the state space, different regions will be visited. The visitation sequence - forthwith referred to as the *itinerary* - can be represented by the letters of the alphabet $\mathcal{A}$. If, as in the example sketched in figure 10.1, the state space is divided into three regions $\mathcal{M}_0$, $\mathcal{M}_1$, and $\mathcal{M}_2$, the "letters" are the integers $\{0, 1, 2\}$, and the itinerary for the trajectory sketched in the figure is $0 \mapsto 2 \mapsto 1 \mapsto 0 \mapsto 1 \mapsto 2 \mapsto \cdots$.

Figure 10.2: Two pinballs that start out very close to each other exhibit the same qualitative dynamics ‗2313‗ for the first three bounces, but due to the exponentially growing separation of trajectories with time, follow different itineraries thereafter: one escapes after ‗2313‗, the other one escapes after ‗23132321‗.
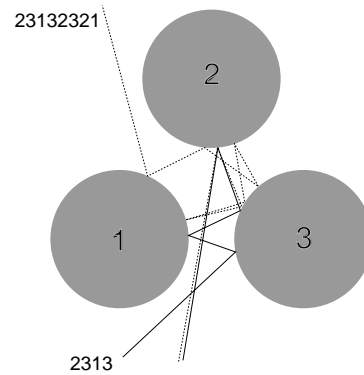
If there is no way to reach partition $\mathcal{M}_i$ from partition $\mathcal{M}_j$, and conversely, partition $\mathcal{M}_j$ from partition $\mathcal{M}_i$, the state space consists of at least two disconnected pieces, and we can analyze it piece by piece. An interesting partition should be dynamically connected, i.e., one should be able to go from any region $\mathcal{M}_i$ to any other region $\mathcal{M}_j$ in a finite number of steps. A dynamical system with such partition is said to be *metrically indecomposable*.

In general one also encounters transient regions - regions to which the dynamics does not return to once they are exited. Hence we have to distinguish between (for us uninteresting) wandering trajectories that never return to the initial neighborhood, and the non–wandering set (2.2) of the *recurrent* trajectories.

The allowed transitions between the regions of a partition are encoded in the $[N \times N]$-dimensional *transition matrix* whose elements take values

$$
T_{ij} \;=\; \begin{cases} 1 & \text{if a transition } \mathcal{M}_j \to \mathcal{M}_i \text{ is possible} \\ 0 & \text{otherwise}. \end{cases} \tag{10.2}
$$

The transition matrix encodes the topological dynamics as an invariant law of motion, with the allowed transitions at any instant independent of the trajectory history, requiring no memory.

Example 10.1 *Complete N-ary dynamics:* *All transition matrix entries equal unity (one can reach any region from any other region in one step):*

$$
T_c = \begin{pmatrix} 1 & 1 & \dots & 1 \\ 1 & 1 & \dots & 1 \\ \vdots & \vdots & \ddots & \vdots \\ 1 & 1 & \dots & 1 \end{pmatrix}. \tag{10.3}
$$

Further examples of transition matrices, such as the 3-disk transition matrix (10.5) and the 1-step memory sparse matrix (10.13), are peppered throughout the text.

However, knowing that a point from $\mathcal{M}_i$ reaches $\mathcal{M}_j$ in one step is not quite good enough. We would be happier if we knew that *any* point in $\mathcal{M}_i$ reaches $\mathcal{M}_j$; otherwise we have to subpartition $\mathcal{M}_i$ into the points which land in $\mathcal{M}_j$, and those which do not, and often we will find ourselves partitioning *ad infinitum*.

Figure 10.3: The 3-disk game of pinball Poincaré section, trajectories emanating from the disk 1 with x_0 = (arclength, parallel momentum) = (s_0, p_0), disk radius : center separation ratio a:R = 1:2.5. (a) Strips of initial points $\mathcal{M}_{12}$, $\mathcal{M}_{13}$ which reach disks 2, 3 in one bounce, respectively. (b) Strips of initial points $\mathcal{M}_{121}$, $\mathcal{M}_{131}$ $\mathcal{M}_{132}$ and $\mathcal{M}_{123}$ which reach disks 1, 2, 3 in two bounces, respectively. (Y. Lan)
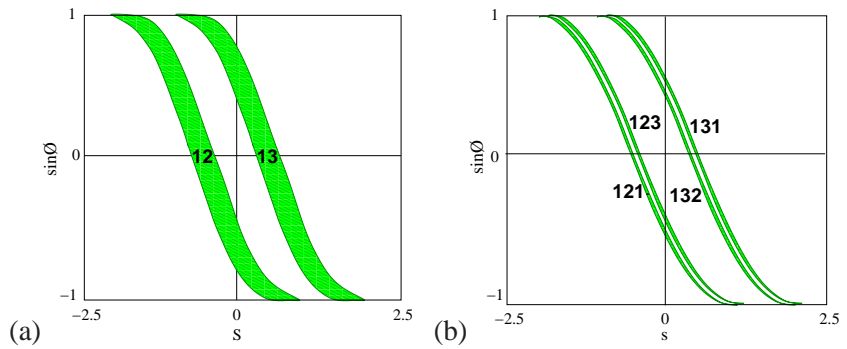
Such considerations motivate the notion of a *Markov partition*, a partition for which no memory of preceding steps is required to fix the transitions allowed in the next step. Dynamically, *finite Markov partitions* can be generated by *expanding* d-dimensional iterated mappings $f : \mathcal{M} \to \mathcal{M}$, if $\mathcal{M}$ can be divided into N regions $\{\mathcal{M}_0, \mathcal{M}_1, \ldots, \mathcal{M}_{N-1}\}$ such that in one step points from an initial region $\mathcal{M}_i$ either fully cover a region $\mathcal{M}_j$, or miss it altogether,

$$\text{either} \quad \mathcal{M}_j \cap f(\mathcal{M}_i) = \emptyset \quad \text{or} \quad \mathcal{M}_j \subset f(\mathcal{M}_i). \tag{10.4}$$

Let us illustrate what this means by our favorite example, the game of pinball.

> **Example 10.2** *3-disk symbolic dynamics:* Consider the motion of a free point particle in a plane with 3 elastically reflecting convex disks. After a collision with a disk a particle either continues to another disk or escapes, and any trajectory can be labeled by the disk sequence. For example, if we label the three disks by 1, 2 and 3, the two trajectories in figure 10.2 have itineraries ‿2313‿, ‿23132321‿ respectively. The 3-disk prime cycles given in figures 9.4 and 11.2 are further examples of such itineraries. [exercise 1.1]
>
> At each bounce a cone of initially nearby trajectories defocuses (see figure 1.8), and in order to attain a desired longer and longer itinerary of bounces the initial point $x_0 = (s_0, p_0)$ has to be specified with a larger and larger precision, and lie within initial state space strips drawn in figure 10.3. Similarly, it is intuitively clear that as we go backward in time (in this case, simply reverse the velocity vector), we also need increasingly precise specification of $x_0 = (s_0, p_0)$ in order to follow a given past itinerary. Another way to look at the survivors after two bounces is to plot $\mathcal{M}_{s_1.s_2}$, the intersection of $\mathcal{M}_{.s_2}$ with the strips $\mathcal{M}_{s_1.}$ obtained by time reversal (the velocity changes sign $\sin\phi \to -\sin\phi$). $\mathcal{M}_{s_1.s_2}$, figure 10.4, is a "rectangle" of nearby trajectories which have arrived from the disk s_1 and are heading for the disk s_2.

The itinerary is finite for a scattering trajectory, coming in from infinity and escaping after a finite number of collisions, infinite for a trapped trajectory, and infinitely repeating for a periodic orbit. A finite length trajectory is not uniquely specified by its finite itinerary, but an isolated unstable cycle is: its itinerary is an infinitely repeating block of symbols. More generally, for hyperbolic flows the intersection of the future and past itineraries, the bi-infinite itinerary $S^-.S^+ = \cdots s_{-2} s_{-1} s_0 . s_1 s_2 s_3 \cdots$ specifies a unique trajectory. This is intuitively clear for our 3-disk game of pinball, and is stated more formally in the definition (10.4) of a Markov partition. The definition requires that the dynamics be expanding forward in time in order to ensure that the cone of trajectories with a given itinerary becomes sharper and sharper as the number of specified symbols is increased.

Figure 10.4: The Poincaré section of the state space for the binary labeled pinball. For definitiveness, this set is generated by starting from disk 1, preceded by disk 2. Indicated are the fixed points $\overline{0}$, $\overline{1}$ and the 2-cycle periodic points $\overline{01}$, $\overline{10}$, together with strips which survive 1, 2, ... bounces. Iteration corresponds to the decimal point shift; for example, all points in the rectangle [01.01] map into the rectangle [010.1] in one iteration. See also figure 11.2 (b).
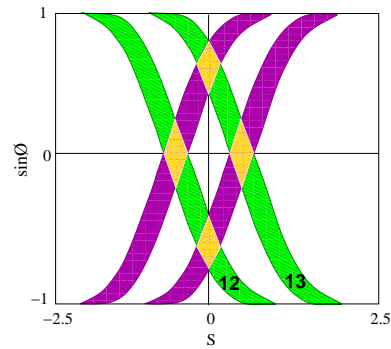
Example 10.3 *Pruning rules for a 3-disk alphabet:*   *As the disks are convex, there can be no two consecutive reflections off the same disk, hence the covering symbolic dynamics consists of all sequences which include no symbol repetitions* 11, 22, 33. *This is a finite set of finite length* pruning rules*, hence, the dynamics is a subshift of finite type (see (10.22) for definition), with the transition matrix (10.2) given by*

$$T \;=\; \begin{pmatrix} 0 & 1 & 1 \\ 1 & 0 & 1 \\ 1 & 1 & 0 \end{pmatrix}. \tag{10.5}$$

For convex disks the separation between nearby trajectories increases at every reflection, implying that the fundamental matrix has an expanding eigenvalue. By the Liouville phase space volume conservation (7.32), the other transverse eigenvalue is contracting. This example demonstrates that finite Markov partitions can be constructed for hyperbolic dynamical systems which are expanding in some directions, contracting in others. Further examples are the 1*-dimensional expanding mapping sketched in figure 10.6, and more examples are worked out in sect. 24.2.*

Determining whether the symbolic dynamics is complete (as is the case for sufficiently separated disks), pruned (for example, for touching or overlapping disks), or only a first coarse graining of the topology (as, for example, for smooth potentials with islands of stability) requires case-by-case investigation, a discussion we postpone to sect. 10.3 and chapter 11. For the time being we assume that the disks are sufficiently separated that there is no additional pruning beyond the prohibition of self-bounces.

If there are no restrictions on symbols, the symbolic dynamics is complete, and *all* binary sequences are admissible itineraries. As this type of symbolic dynamics pops up frequently, we list the shortest binary prime cycles in table 10.1.

[exercise 10.2]

Inspecting the figure 10.3 we see that the relative ordering of regions with differing finite itineraries is a qualitative, topological property of the flow, so it makes sense to define a simple "canonical" representative partition which in a simple manner exhibits spatial ordering common to an entire class of topologically similar nonlinear flows.

in depth:
chapter 19, p. 320

Table 10.1: Prime cycles for the binary symbolic dynamics up to length 9.

n_p	p	n_p	p	n_p	p	n_p	p	n_p	p
1	0	7	0001001	8	00001111	9	000001101	9	001001111
	1		0000111		00010111		000010011		001010111
2	01		0001011		00011011		000010101		001011011
3	001		0001101		00011101		000011001		001011101
	011		0010011		00100111		000100011		001100111
4	0001		0010101		00101011		000100101		001101011
	0011		0001111		00101101		000101001		001101101
	0111		0010111		00110101		000001111		001110101
5	00001		0011011		00011111		000010111		010101011
	00011		0011101		00101111		000011011		000111111
	00101		0101011		00110111		000011101		001011111
	00111		0011111		00111011		000100111		001101111
	01011		0101111		00111101		000101011		001110111
	01111		0110111		01010111		000101101		001111011
6	000001		0111111		01011011		000110011		001111101
	000011	8	00000001		00111111		000110101		010101111
	000101		00000011		01011111		000111001		010110111
	000111		00000101		01101111		001001011		010111011
	001011		00001001		01111111		001001101		001111111
	001101		00000111	9	000000001		001010011		010111111
	001111		00001011		000000011		001010101		011011111
	010111		00001101		000000101		000011111		011101111
	011111		00010011		000001001		000101111		011111111
7	0000001		00010101		000010001		000110111		
	0000011		00011001		000000111		000111011		
	0000101		00100101		000001011		000111101		

10.2   Stretch and fold

Symbolic dynamics for *N*-disk game of pinball is so straightforward that one may altogether fail to see the connection between the topology of hyperbolic flows and their symbolic dynamics. This is brought out more clearly by the 1-dimensional visualization of "stretch & fold" flows to which we turn now.

Suppose concentrations of certain chemical reactants worry you, or the variations in the Chicago temperature, humidity, pressure and winds affect your mood. All such properties vary within some fixed range, and so do their rates of change. Even if we are studying an open system such as the 3-disk pinball game, we tend to be interested in a finite region around the disks and ignore the escapees. So a typical dynamical system that we care about is *bounded*. If the price for keeping going is high - for example, we try to stir up some tar, and observe it come to a dead stop the moment we cease our labors - the dynamics tends to settle into a simple limiting state. However, as the resistance to change decreases - the tar is heated up and we are more vigorous in our stirring - the dynamics becomes unstable.

If a flow is locally unstable but globally bounded, any open ball of initial points will be stretched out and then folded back.

At this juncture we show how this works on the simplest example: unimodal mappings of the interval. The erudite reader should skim through this chapter and then take a more demanding path, via the Smale horseshoes of chapter 11.
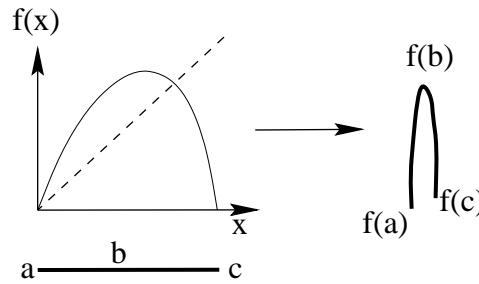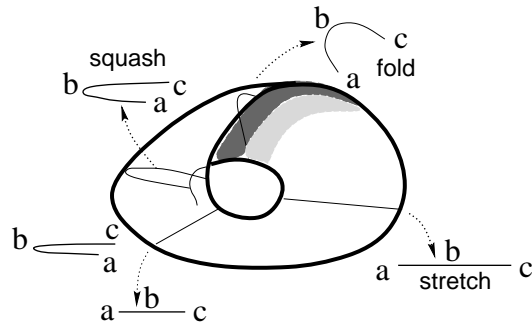
Figure 10.5: (a) A recurrent flow that stretches and folds. (b) The "stretch & fold" return map on the Poincaré section.   (a)

Unimodal maps are easier, but physically less motivated. The Smale horseshoes are the high road, more complicated, but the right tool to generalize what we learned from the 3-disk dynamics, and begin analysis of general dynamical systems. It is up to you - unimodal maps suffice to get quickly to the heart of this treatise.

### 10.2.1 Temporal ordering: itineraries

In this section we learn how to *name* (and, in chapter 13, how to *count*) periodic orbits for the simplest, and nevertheless very instructive case, for 1-dimensional maps of an interval.

Suppose that the compression of the folded interval in figure 10.5 is so fierce that we can neglect the thickness of the attractor. For example, the Rössler flow (2.17) is volume contracting, and an interval transverse to the attractor is stretched, folded and pressed back into a nearly 1-dimensional interval, typically compressed transversally by a factor of $\approx 10^{13}$ in one Poincaré section return. In such cases it makes sense to approximate the return map of a "stretch & fold" flow by a 1-dimensional map.

The simplest mapping of this type is *unimodal;* interval is stretched and folded only once, with at most two points mapping into a point in the refolded interval. A unimodal map $f(x)$ is a 1-dimensional function $\mathbb{R} \to \mathbb{R}$ defined on an interval $\mathcal{M} \in \mathbb{R}$ with a monotonically increasing (or decreasing) branch, a *critical point* (or interval) x_c for which $f(x_c)$ attains the maximum (minimum) value, followed by a monotonically decreasing (increasing) branch. *Uni*-modal means that the map is a 1-humped map with one critical point within interval $\mathcal{M}$. A *multi*-modal map has several critical points within interval $\mathcal{M}$.

Example 10.4 *Complete tent map, quadratic map:*   *The simplest examples of*

Figure 10.6: (a) The complete tent map together with intervals that follow the indicated itinerary for *n* steps.   (b) A unimodal repeller with the remaining intervals after 1, 2 and 3 iterations. Intervals marked $s_1 s_2 \cdots s_n$ are unions of all points that do not escape in *n* iterations, and follow the itinerary $S^+ = s_1 s_2 \cdots s_n$. Note that the spatial ordering does not respect the binary ordering; for example $x_{00} < x_{01} < x_{11} < x_{10}$. Also indicated: the fixed points x_0, x_1, the 2-cycle $\overline{01}$, and the 3-cycle $\overline{011}$.
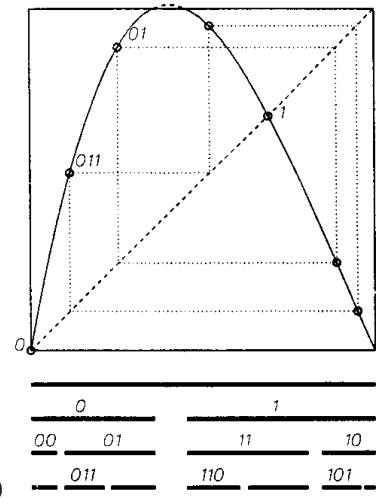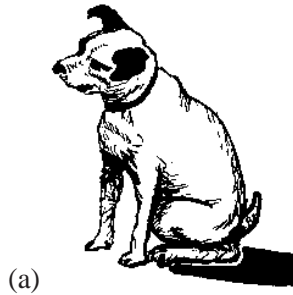
unimodal maps are the complete tent map, *figure 10.6 (a),*

$$f(\gamma) = 1 - 2|\gamma - 1/2|\,, \tag{10.6}$$

and the quadratic map (sometimes also called the logistic map*)*

$$x_{t+1} = 1 - ax_t^2\,, \tag{10.7}$$

with the one critical point at $x_c = 0$. Further examples are the repelling unimodal map of figure 10.6 (b) and the piecewise linear tent map (10.6).

Such dynamical systems are irreversible (the inverse of f is double-valued), but, as we shall show in sect. 11.3, they may nevertheless serve as effective descriptions of invertible 2-dimensional hyperbolic flows.

For the unimodal maps of figure 10.6 a Markov partition of the unit interval $\mathcal{M}$ is given by the two intervals $\{\mathcal{M}_0, \mathcal{M}_1\}$. We refer to (10.6) as the "complete" tent map because its symbolic dynamics is complete binary: as both $f(\mathcal{M}_0)$ and $f(\mathcal{M}_1)$ fully cover $\mathcal{M}_0$ and $\mathcal{M}_1$, the corresponding transition matrix is a [2×2] matrix with all entries equal to 1, as in (10.3). As binary symbolic dynamics pops up frequently in applications, we list the shortest binary prime cycles in table 10.1.

Example 10.5 _Lorenz flow: a 1–d return map_   *We now deploy the symmetry of Lorenz flow to streamline and complete analysis of the Lorenz strange attractor commenced in example 9.2.*

The dihedral $D_1 = \{e, R\}$ symmetry identifies the two equilibria EQ_1 and EQ_2, and the traditional "two-eared" Lorenz flow figure 2.4 is replaced by the "single-eared" flow of figure 9.2 (a). Furthermore, symmetry identifies two sides of any plane through the z axis, replacing a full-space Poincaré section plane by a half-plane, and the two directions of a full-space eigenvector of EQ_0 by a one-sided eigenvector, see figure 9.2 (a).

Example 4.7 explained the genesis of the x_{EQ1} equilibrium unstable manifold, its orientation and thickness, its collision with the z-axis, and its heteroclinic connection to the $x_{EQ0} = (0, 0, 0)$ equilibrium. All that remains is to describe how the EQ_0 neighborhood connects back to the EQ_1 unstable manifold. Figure 9.2 now shows clearly how the Lorenz dynamics is pieced together from the 2 equilibria and their unstable manifolds:

Having completed the descent to EQ_0, the infinitesimal neighborhood of the heteroclinic $EQ_1 \rightarrow EQ_0$ trajectory is ejected along the unstable manifold of EQ_0 and is
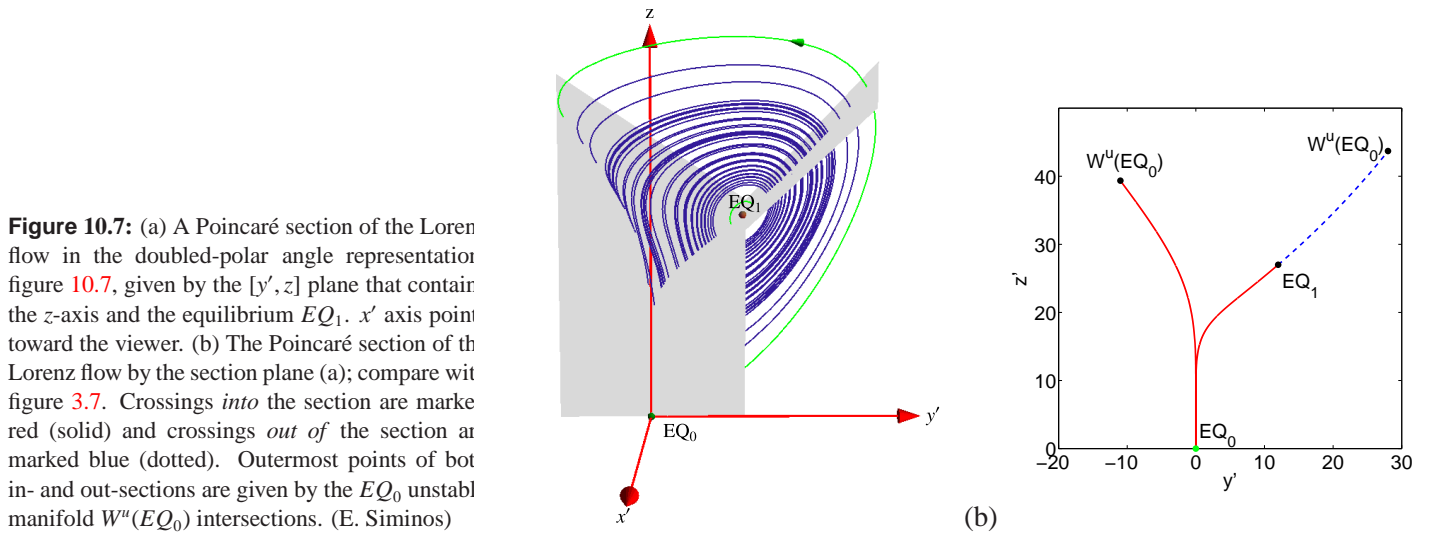
Figure 10.7: (a) A Poincaré section of the Lorenz flow in the doubled-polar angle representation figure 10.7, given by the $[y', z]$ plane that contains the z-axis and the equilibrium EQ_1. x' axis points toward the viewer. (b) The Poincaré section of the Lorenz flow by the section plane (a); compare with figure 3.7. Crossings *into* the section are marked red (solid) and crossings *out of* the section are marked blue (dotted). Outermost points of both in- and out-sections are given by the EQ_0 unstable manifold $W^u(EQ_0)$ intersections. (E. Siminos)

Figure 10.8: The Poincaré return map $s_{n+1} = P(s_n)$ parameterized by Euclidean arclength s measured along the EQ_1 unstable manifold, from x_{EQ1} to $W^u(EQ_0)$ section point, uppermost right point of the blue segment in figure 10.7 (b). The critical point (the "crease") of the map is given by the section of the heteroclinic orbit $W^s(EQ_0)$ that descends all the way to EQ_0, in infinite time and with infinite slope. (E. Siminos)
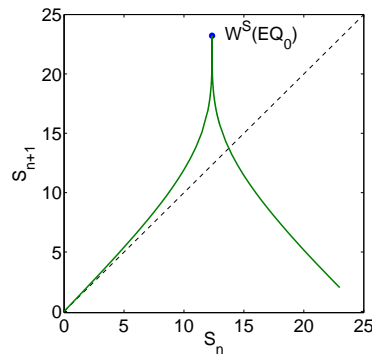
re-injected into the unstable manifold of EQ_1. Both sides of the narrow strip enclosing the EQ_0 unstable manifold lie above it, and they get folded onto each other with a knife-edge crease (contracted exponentially for infinite time at the EQ_0 heteroclinic point), with the heteroclinic out-trajectory defining the outer edge of the strange attractor. This leads to the folding of the outer branch of the Lorenz strange attractor, illustrated in the figure 10.7 (b), with the outermost edge following the unstable manifold of EQ_0.

Now the stage is set for construction of Poincaré sections and associated Poincaré return maps. There are two natural choices; the section at EQ_0, lower part of figure 10.7 (b), and the section (blue) above EQ_1. The first section, together with the blowup of the EQ_0 neighborhood, figure 4.7 (b), illustrates clearly the scarcity of trajectories (vanishing natural measure) in the neighborhood of EQ_0. The flat section above EQ_1 (which is, believe it or not, a smooth conjugacy by the flow of the knife-sharp section at EQ_0) is more convenient for our purposes. Its return map is given by figure 10.8.

The rest is straight sailing: to accuracy 10^{-4} the return map is unimodal, its "critical" point's forward trajectory yields the kneading sequence, and the admissible binary sequences, so any number of cycle points can be accurately determined from this 1-dimensional return map, and the 3-d cycles then verified by integrating the Lorenz differential equations (2.12). The map is everywhere expanding on the strange attractor, so it is no wonder mathematicians can here make the ergodicity rigorous.

Finally, the relation between the full state space periodic orbits, and the fundamental domain (9.16) reduced orbits: Full state space cycle pairs p, Rp map into a single cycles $\tilde{p}$ in the fundamental domain, and any self-dual cycle $p = Rp = \tilde{p}R\tilde{p}$ is a repeat of a relative periodic orbit $\tilde{p}$.

> *But there is* trouble in paradise. *By a fluke, the Lorenz attractor, the first flow to popularize strange attractors, turns to be topologically one of the simplest strange attractors. But it is not "uniformly hyperbolic." The flow near EQ_1 is barely unstable, while the flow near EQ_0 is arbitrarily unstable. So binary enumeration of cycles mixes cycles of vastly different stabilities, and is not very useful - presumably the practical way to compute averages is by stability ordering.*
>
> *(E. Siminos and J. Halcrow)*

The *critical value* denotes either the maximum or the minimum value of $f(x)$ on the defining interval; we assume here that it is a maximum, $f(x_c) \geq f(x)$ for all $x \in \mathcal{M}$. The critical value $f(x_c)$ belongs neither to the left nor to the right partition $\mathcal{M}_i$, and is denoted by its own symbol $s = C$. As we shall see, its preimages serve as partition boundary points.

The trajectory $x_1, x_2, x_3, \ldots$ of the initial point x_0 is given by the iteration $x_{n+1} = f(x_n)$. Iterating f and checking whether the point lands to the left or to the right of x_c generates a *temporally* ordered topological itinerary (10.15) for a given trajectory,

$$
s_n = \begin{cases} 1 & \text{if } x_n > x_c \\ 0 & \text{if } x_n < x_c \end{cases} .
\tag{10.8}
$$

We shall refer to $S^+(x_0) = .s_1 s_2 s_3 \cdots$ as the *future itinerary*. Our next task is to answer the reverse problem: given an itinerary, what is the corresponding *spatial* ordering of points that belong to a given trajectory?

10.2.2   Spatial ordering, 1-d maps

> Tired of being harassed by your professors? Finish, get a job, do combinatorics your own way, while you still know everything.
> —Professor Gatto Nero

Suppose you have succeeded in constructing a covering symbolic dynamics, such as for a well-separated 3-disk system. Now start moving the disks toward each other. At some critical separation a disk will start blocking families of trajectories traversing the other two disks. The order in which trajectories disappear is determined by their relative ordering in space; the ones closest to the intervening disk will be pruned first. Determining inadmissible itineraries requires that we relate the spatial ordering of trajectories to their time ordered itineraries.

[exercise 11.8]

The easiest point of departure is to start out by working out this relation for the symbolic dynamics of 1-dimensional mappings. As it appears impossible to present this material without getting bogged down in a sea of 0's, 1's and subscripted subscripts, we announce the main result before embarking upon its derivation:

[section 10.3]

The admissibility criterion eliminates *all* itineraries that cannot occur for a given unimodal map.

Figure 10.9: Alternating binary tree relates the itinerary labeling of the unimodal map figure 10.6 intervals to their spatial ordering. Dotted line stands for 0, full line for 1; the binary sub-tree whose root is a full line (symbol 1) reverses the orientation, due to the orientation reversing fold in figures 10.5 and 10.6.
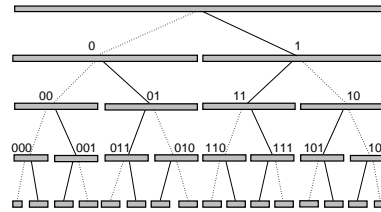
The tent map (10.6) consists of two straight segments joined at $x = 1/2$. The symbol s_n defined in (10.8) equals 0 if the function increases, and 1 if the function decreases. The piecewise linearity of the map makes it possible to analytically determine an initial point given its itinerary, a property that we now use to define a topological coordinatization common to all unimodal maps.

Here we have to face the fundamental problem of pedagogy: combinatorics cannot be taught. The best one can do is to state the answer, and then hope that you will figure it out by yourself. Once you figure it out, feel free to complain that the way the rule is stated here is incomprehensible, and shows us how you did it better.

The tent map point $\gamma(S^+)$ with future itinerary S^+ is given by converting the sequence of s_n's into a binary number by the following algorithm:

$$
\begin{aligned}
w_{n+1} &= \begin{cases} w_n & \text{if } s_{n+1} = 0 \\ 1 - w_n & \text{if } s_{n+1} = 1 \end{cases}, \qquad w_1 = s_1 \\
\gamma(S^+) &= 0.w_1 w_2 w_3 \ldots = \sum_{n=1}^{\infty} w_n/2^n .
\end{aligned}
\tag{10.9}
$$

This follows by inspection from the binary tree of figure 10.9.

[exercise 10.4]

Example 10.6 *Converting γ to S^+:* *γ whose itinerary is $S^+ = 0110000 \cdots$ is given by the binary number $\gamma = .010000 \cdots$. Conversely, the itinerary of $\gamma = .01$ is $s_1 = 0$, $f(\gamma) = .1 \rightarrow s_2 = 1$, $f^2(\gamma) = f(.1) = 1 \rightarrow s_3 = 1$, etc..*

We shall refer to $\gamma(S^+)$ as the *(future) topological coordinate*. w_t's are the digits in the binary expansion of the starting point γ for the complete tent map (10.6). In the left half-interval the map $f(x)$ acts by multiplication by 2, while in the right half-interval the map acts as a flip as well as multiplication by 2, reversing the ordering, and generating in the process the sequence of s_n's from the binary digits w_n.

The mapping $\qquad x_0 \rightarrow S^+(x_0) \rightarrow \gamma_0 = \gamma(S^+) \qquad$ is a *topological conjugacy* which maps the trajectory of an initial point x_0 under iteration of a given unimodal map to that initial point γ for which the trajectory of the "canonical" unimodal map (10.6) has the same itinerary. The virtue of this conjugacy is that it *preserves the ordering* for any unimodal map in the sense that if $\overline{x} > x$, then $\overline{\gamma} > \gamma$.

Figure 10.10:   The "dike" map obtained by slicing of a top portion of the tent map figure 10.6 (a). Any orbit that visits the primary pruning interval $(\kappa, 1]$ is inadmissible.   The admissible orbits form the Cantor set obtained by removing from the unit interval the primary pruning interval and all its iterates. Any admissible orbit has the same topological coordinate and itinerary as the corresponding tent map figure 10.6 (a) orbit.

10.3   Kneading theory

(K.T. Hansen and P. Cvitanović)

The main motivation for being mindful of spatial ordering of temporal itineraries is that this spatial ordering provides us with criteria that separate inadmissible orbits from those realizable by the dynamics. For 1-dimensional mappings the *kneading theory* provides such criterion of admissibility.

If the parameter in the quadratic map (10.7) is $a > 2$, then the iterates of the critical point x_c diverge for $n \to \infty$. As long as $a \geq 2$, any sequence S^+ composed of letters $s_i = \{0, 1\}$ is admissible, and any value of $0 \leq \gamma < 1$ corresponds to an admissible orbit in the non–wandering set of the map. The corresponding repeller is a complete binary labeled Cantor set, the $n \to \infty$ limit of the nth level covering intervals sketched in figure 10.6.

For $a < 2$ only a subset of the points in the interval $\gamma \in [0, 1]$ corresponds to admissible orbits. The forbidden symbolic values are determined by observing that the largest x_n value in an orbit $x_1 \to x_2 \to x_3 \to \dots$ has to be smaller than or equal to the image of the critical point, *the critical value* $f(x_c)$. Let $K = S^+(x_c)$ be the itinerary of the critical point x_c, denoted the *kneading sequence* of the map. The corresponding topological coordinate is called the *kneading value*

$$\kappa = \gamma(K) = \gamma(S^+(x_c)). \tag{10.10}$$

A map with the same kneading sequence K as $f(x)$, such as the dike map figure 10.10, is obtained by slicing off all $\gamma(S^+(x_0)) > \kappa$,

$$f(\gamma) = \begin{cases} f_0(\gamma) = 2\gamma & \gamma \in I_0 = [0, \kappa/2) \\ f_c(\gamma) = \kappa & \gamma \in I_c = [\kappa/2, 1 - \kappa/2] \\ f_1(\gamma) = 2(1 - \gamma) & \gamma \in I_1 = [1 - \kappa/2, 1] \end{cases} . \tag{10.11}$$

The dike map is the complete tent map figure 10.6 (a) with the top sliced off. It is convenient for coding the symbolic dynamics, as those γ values that survive the

pruning are the same as for the complete tent map figure 10.6 (a), and are easily converted into admissible itineraries by (10.9).

If $\gamma(S^+) > \gamma(K)$, the point x whose itinerary is S^+ would exceed the critical value, $x > f(x_c)$, and hence cannot be an admissible orbit. Let

$$\hat{\gamma}(S^+) = \sup_m \gamma(\sigma^m(S^+)) \tag{10.12}$$

be the *maximal value*, the highest topological coordinate reached by the orbit $x_1 \to x_2 \to x_3 \to \ldots$. We shall call the interval $(\kappa, 1]$ the *primary pruned interval*. The orbit S^+ is inadmissible if γ of any shifted sequence of S^+ falls into this interval.

Criterion of admissibility: *Let κ be the kneading value of the critical point, and $\hat{\gamma}(S^+)$ be the maximal value of the orbit S^+. Then the orbit S^+ is admissible if and only if $\hat{\gamma}(S^+) \leq \kappa$.*

While a unimodal map may depend on many arbitrarily chosen parameters, its dynamics determines the unique kneading value κ. We shall call κ the *topological parameter* of the map. Unlike the parameters of the original dynamical system, the topological parameter has no reason to be either smooth or continuous. The jumps in κ as a function of the map parameter such as a in (10.7) correspond to inadmissible values of the topological parameter. Each jump in κ corresponds to a stability window associated with a stable cycle of a smooth unimodal map. For the quadratic map (10.7) κ increases monotonically with the parameter a, but for a general unimodal map such monotonicity need not hold.

For further details of unimodal dynamics, the reader is referred to appendix D.1. As we shall see in sect. 11.5, for higher dimensional maps and flows there is no single parameter that orders dynamics monotonically; as a matter of fact, there is an infinity of parameters that need adjustment for a given symbolic dynamics. This difficult subject is beyond our current ambition horizon.

10.4   Markov graphs

10.4.1   Finite memory

In the complete N-ary symbolic dynamics case (see example (10.3)) the choice of the next symbol requires no memory of the previous ones. However, any further refinement of the partition requires finite memory.

For example, for the binary labeled repeller with complete binary symbolic dynamics, we might chose to partition the state space into four regions $\{\mathcal{M}_{00}, \mathcal{M}_{01}, \mathcal{M}_{10}, \mathcal{M}_{11}\}$, a 1-step refinement of the initial partition $\{\mathcal{M}_0, \mathcal{M}_1\}$. Such partitions are drawn in figure 10.4, as well as figure 1.9. Topologically f acts as a left shift (11.10), and its action on the rectangle $[.01]$ is to move the decimal point to the right, to

Figure 10.11: (a) The self-similarity of the complete binary symbolic dynamics represented by a binary tree (b) identification of nodes $B = A$, $C = A$ leads to the finite 1-node, 2-links Markov graph. All admissible itineraries are generated as walks on this finite Markov graph.
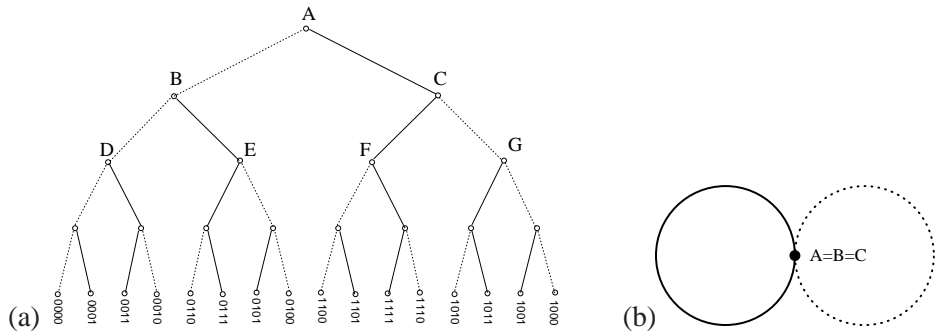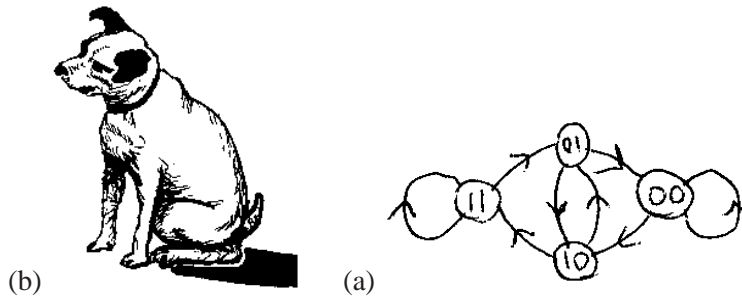

Figure 10.12: (a) The 2-step memory Markov graph, links version obtained by identifying nodes $A = D = E = F = G$ in figure 10.11 (a). Links of this graph correspond to the matrix entries in the transition matrix (10.13). (b) the 2-step memory Markov graph, node version.

[0.1], forget the past, [.1], and land in either of the two rectangles $\{[.10], [.11]\}$. Filling in the matrix elements for the other three initial states we obtain the 1-step memory transition matrix acting on the 4-state vector

[exercise 10.7]

$$\phi' = T\phi = \begin{pmatrix} T_{00,00} & 0 & T_{00,10} & 0 \\ T_{01,00} & 0 & T_{01,10} & 0 \\ 0 & T_{10,01} & 0 & T_{10,11} \\ 0 & T_{11,01} & 0 & T_{11,11} \end{pmatrix} \begin{pmatrix} \phi_{00} \\ \phi_{01} \\ \phi_{10} \\ \phi_{11} \end{pmatrix}. \tag{10.13}$$

By the same token, for M-step memory the only nonvanishing matrix elements are of the form $T_{s_1 s_2 \ldots s_{M+1}, s_0 s_1 \ldots s_M}$, $s_{M+1} \in \{0, 1\}$. This is a sparse matrix, as the only non vanishing entries in the $m = s_0 s_1 \ldots s_M$ column of T_{dm} are in the rows $d = s_1 \ldots s_M 0$ and $d = s_1 \ldots s_M 1$. If we increase the number of steps remembered, the transition matrix grows big quickly, as the N-ary dynamics with M-step memory requires an $[N^{M+1} \times N^{M+1}]$ matrix. Since the matrix is very sparse, it pays to find a compact representation for T. Such representation is afforded by Markov graphs, which are not only compact, but also give us an intuitive picture of the topological dynamics.
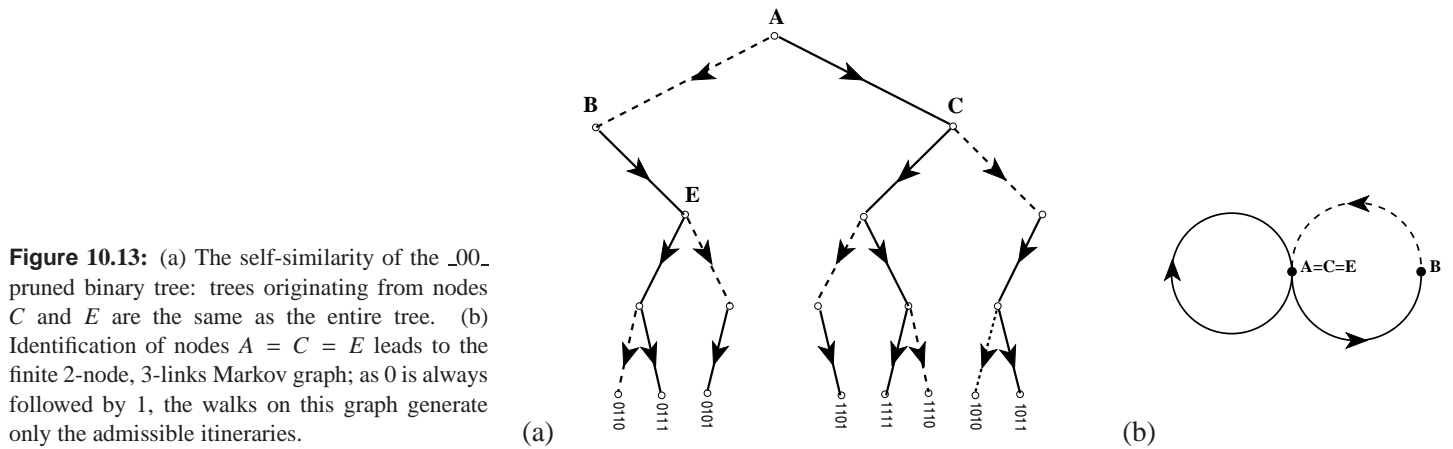
[exercise 13.1]

Construction of a good Markov graph is, like combinatorics, unexplainable. The only way to learn is by some diagrammatic gymnastics, so we work our way through a sequence of exercises in lieu of plethora of baffling definitions.

[exercise 13.4]
[exercise 13.1]

To start with, what do finite graphs have to do with infinitely long trajectories? To understand the main idea, let us construct a graph that enumerates all possible itineraries for the case of complete binary symbolic dynamics.

Mark a dot "·" on a piece of paper. Draw two short lines out of the dot, end each with a dot. The full line will signify that the first symbol in an itinerary is "1", and the dotted line will signifying "0". Repeat the procedure for each of the

Figure 10.13: (a) The self-similarity of the _00_ pruned binary tree: trees originating from nodes C and E are the same as the entire tree. (b) Identification of nodes $A = C = E$ leads to the finite 2-node, 3-links Markov graph; as 0 is always followed by 1, the walks on this graph generate only the admissible itineraries.

(a)   (b)

two new dots, and then for the four dots, and so on. The result is the binary tree of figure 10.11 (a). Starting at the top node, the tree enumerates exhaustively all distinct finite itineraries

$$\{0, 1\},$$
$$\{00, 01, 10, 11\},$$
$$\{000, 001, 010, \cdots\}, \cdots .$$

The $M = 4$ nodes in figure 10.11 (a) correspond to the 16 distinct binary strings of length 4, and so on. By habit we have drawn the tree as the alternating binary tree of figure 10.9, but that has no significance as far as enumeration of itineraries is concerned - an ordinary binary tree would serve just as well.

The trouble with an infinite tree is that it does not fit on a piece of paper. On the other hand, we are not doing much - at each node we are turning either left or right. Hence all nodes are equivalent, and can be identified. To say it in other words, the tree is self-similar; the trees originating in nodes B and C are themselves copies of the entire tree. The result of identifying $B = A$, $C = A$ is a single node, 2-link Markov graph of figure 10.11 (b): any itinerary generated by the binary tree figure 10.11 (a), no matter how long, corresponds to a walk on this graph.

This is the most compact encoding of the complete binary symbolic dynamics. Any number of more complicated Markov graphs can do the job as well, and might be sometimes preferable. For example, identifying the trees originating in D, E, F and G with the entire tree leads to the 2-step memory Markov graph of figure 10.12a. The corresponding transition matrix is given by (10.13).

in depth:
chapter 11, p. 174

fast track:
chapter 13, p. 212

10.5 Symbolic dynamics, basic notions

In this section we collect the basic notions and definitions of symbolic dynamics. The reader might prefer to skim through this material on first reading, return to it later as the need arises.

Shifts. We associate with every initial point $x_0 \in \mathcal{M}$ the *future itinerary*, a sequence of symbols $S^+(x_0) = s_1 s_2 s_3 \cdots$ which indicates the order in which the regions are visited. If the trajectory $x_1, x_2, x_3, \ldots$ of the initial point x_0 is generated by

$$x_{n+1} = f(x_n), \tag{10.14}$$

then the itinerary is given by the symbol sequence

$$s_n = s \qquad \text{if} \qquad x_n \in \mathcal{M}_s F. \tag{10.15}$$

Similarly, the *past itinerary* $S^-(x_0) = \cdots s_{-2} s_{-1} s_0$ describes the history of x_0, the order in which the regions were visited before arriving to the point x_0. To each point x_0 in the dynamical space we thus associate a bi-infinite itinerary

$$S(x_0) = (s_k)_{k \in \mathbb{Z}} = S^-.S^+ = \cdots s_{-2} s_{-1} s_0.s_1 s_2 s_3 \cdots. \tag{10.16}$$

The itinerary will be finite for a scattering trajectory, entering and then escaping $\mathcal{M}$ after a finite time, infinite for a trapped trajectory, and infinitely repeating for a periodic trajectory.

The set of all bi-infinite itineraries that can be formed from the letters of the alphabet $\mathcal{A}$ is called the *full shift*

$$\mathcal{A}^{\mathbb{Z}} = \{(s_k)_{k \in \mathbb{Z}} : s_k \in \mathcal{A} \text{ for all k } \in \mathbb{Z}\}. \tag{10.17}$$

The jargon is not thrilling, but this is how professional dynamicists talk to each other. We will stick to plain English to the extent possible.

We refer to this set of all conceivable itineraries as the *covering* symbolic dynamics. The name *shift* is descriptive of the way the dynamics acts on these sequences. As is clear from the definition (10.15), a forward iteration $x \rightarrow x' = f(x)$ shifts the entire itinerary to the left through the "decimal point." This operation, denoted by the shift operator σ,

$$\sigma(\cdots s_{-2} s_{-1} s_0.s_1 s_2 s_3 \cdots) = \cdots s_{-2} s_{-1} s_0 s_1.s_2 s_3 \cdots, \tag{10.18}$$

demoting the current partition label s_1 from the future S^+ to the "has been" itinerary S^-. The inverse shift σ^{-1} shifts the entire itinerary one step to the right.

A finite sequence $b = s_k s_{k+1} \cdots s_{k+n_b-1}$ of symbols from $\mathcal{A}$ is called a *block* of length n_b. A state space trajectory is *periodic* if it returns to its initial point after a finite time; in the shift space the trajectory is periodic if its itinerary is an infinitely repeating block p^∞. We shall refer to the set of periodic points that belong to a given periodic orbit as a *cycle*

$$p = \overline{s_1 s_2 \cdots s_{n_p}} = \{x_{s_1 s_2 \cdots s_{n_p}}, x_{s_2 \cdots s_{n_p} s_1}, \cdots, x_{s_{n_p} s_1 \cdots s_{n_p-1}}\}. \tag{10.19}$$

By its definition, a cycle is invariant under cyclic permutations of the symbols in the repeating block. A bar over a finite block of symbols denotes a periodic itinerary with infinitely repeating basic block; we shall omit the bar whenever it is clear from the context that the trajectory is periodic. Each *cycle point* is labeled by the first n_p steps of its future itinerary. For example, the 2nd cycle point is labeled by

$$x_{s_2 \cdots s_{n_p} s_1} = x_{\overline{s_2 \cdots s_{n_p} s_1} \cdot s_2 \cdots s_{n_p} s_1}.$$

A *prime* cycle p of length n_p is a single traversal of the orbit; its label is a block of n_p symbols that cannot be written as a repeat of a shorter block (in literature such cycle is sometimes called *primitive*; we shall refer to it as "prime" throughout this text).

Partitions. A partition is called *generating* if every infinite symbol sequence corresponds to a distinct point in the state space. Finite Markov partition (10.4) is an example. Constructing a generating partition for a given system is a difficult problem. In examples to follow we shall concentrate on cases which allow finite partitions, but in practice almost any generating partition of interest is infinite.

A mapping $f : \mathcal{M} \to \mathcal{M}$ together with a partition $\mathcal{A}$ induces *topological dynamics* (Σ, σ), where the *subshift*

$$\Sigma = \{(s_k)_{k\in\mathbb{Z}}\}, \tag{10.20}$$

is the set of all *admissible* infinite itineraries, and $\sigma : \Sigma \to \Sigma$ is the shift operator (10.18). The designation "subshift" comes form the fact that $\Sigma \subset \mathcal{A}^{\mathbb{Z}}$ is the subset of the full shift (10.17). One of our principal tasks in developing symbolic dynamics of dynamical systems that occur in nature will be to determine Σ, the set of all bi-infinite itineraries S that are actually realized by the given dynamical system.

A partition too coarse, coarser than, for example, a Markov partition, would assign the same symbol sequence to distinct dynamical trajectories. To avoid that, we often find it convenient to work with partitions finer than strictly necessary. Ideally the dynamics in the refined partition assigns a unique infinite itinerary $\cdots s_{-2} s_{-1} s_0.s_1 s_2 s_3 \cdots$ to each distinct trajectory, but there might exist full shift symbol sequences (10.17) which are not realized as trajectories; such sequences are called *inadmissible*, and we say that the symbolic dynamics is *pruned*. The

word is suggested by "pruning" of branches corresponding to forbidden sequences for symbolic dynamics organized hierarchically into a tree structure, as explained in sect. 10.4.

Pruning. If the dynamics is pruned, the alphabet must be supplemented by a *grammar*, a set of pruning rules. After the inadmissible sequences have been pruned, it is often convenient to parse the symbolic strings into words of variable length - this is called *coding*. Suppose that the grammar can be stated as a finite number of pruning rules, each forbidding a block of finite length,

$$\mathcal{G} = \{b_1, b_2, \cdots b_k\} , \tag{10.21}$$

where a *pruning block* b is a sequence of symbols $b = s_1 s_2 \cdots s_{n_b}$, $s \in \mathcal{A}$, of finite length n_b. In this case we can always construct a finite Markov partition (10.4) by replacing finite length words of the original partition by letters of a new alphabet. In particular, if the longest forbidden block is of length $M + 1$, we say that the symbolic dynamics is a shift of finite type with M-step memory. In that case we can *recode* the symbolic dynamics in terms of a new alphabet, with each new letter given by an admissible block of at most length M. In the new alphabet the grammar rules are implemented by setting $T_{ij} = 0$ in (10.3) for forbidden transitions.

A topological dynamical system (Σ, σ) for which all admissible itineraries are generated by a finite transition matrix

$$\Sigma = \{(s_k)_{k\in\mathbb{Z}} \ : \ T_{s_k s_{k+1}} = 1 \quad \text{for all } k\} \tag{10.22}$$
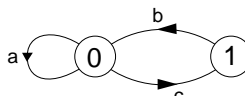
is called a subshift of *finite type*. Such systems are particularly easy to handle; the topology can be converted into symbolic dynamics by representing the transition matrix by a finite directed *Markov graph*, a convenient visualization of topological dynamics.

Markov graphs. A Markov graph describes compactly the ways in which the state space regions map into each other, accounts for finite memory effects in dynamics, and generates the totality of admissible trajectories as the set of all possible walks along its links.

A Markov graph consists of a set of *nodes* (or *vertices*, or *states*), one for each state in the alphabet $\mathcal{A} = \{A, B, C, \cdots, Z\}$, connected by a set of directed *links* (*edges*, *arcs*). Node i is connected by a directed link to node j whenever the transition matrix element (10.2) takes value $T_{ij} = 1$. There might be a set of links connecting two nodes, or links that originate and terminate on the same node. Two graphs are isomorphic if one can be obtained from the other by relabeling links and nodes; for us they are one and the same graph. As we are interested in recurrent dynamics, we restrict our attention to *irreducible* or *strongly connected* graphs, i.e., graphs for which there is a path from any node to any other node.

> **Example 10.7** *"Golden mean" pruning*   Consider a simple subshift on two-state partition $\mathcal{A} = \{0, 1\}$, with the simplest grammar $\mathcal{G}$ possible: a single pruning block $b =$

Figure 10.14: (a) The transition matrix for binary alphabet $\mathcal{A} = \{0, 1\}$, $b = \_11\_$ pruned. (b) The corresponding Markov graph.

$$T = \begin{pmatrix} 1 & 1 \\ 1 & 0 \end{pmatrix} \text{(b)}$$

$\_11\_$ *(consecutive repeat of symbol* 1 *is inadmissible): the state* $\mathcal{M}_0$ *maps both onto* $\mathcal{M}_0$ *and* $\mathcal{M}_1$*, but the state* $\mathcal{M}_1$ *maps only onto* $\mathcal{M}_0$*. The transition matrix for this grammar is given in figure* 10.14 *(a). The corresponding finite 2-node, 3-links Markov graph, with nodes coding the symbols, is given in figure* 10.14 *(b). All admissible itineraries are generated as walks on this finite Markov graph.*

in depth:
chapter 11, p. 174

Résumé

In chapters 16 and 17 we will establish that spectra of evolution operators can be extracted from periodic orbit sums:

$$\sum (\text{spectral eigenvalues}) = \sum (\text{periodic orbits}) .$$

In order to implement this theory we need to know what periodic orbits can exist, and the symbolic dynamics developed above and in chapter 11 is an invaluable tool toward this end.

Commentary

Remark 10.1 Symbolic dynamics, history and good taste.   For a brief history of symbolic dynamics, from J. Hadamard in 1898 onward, see Notes to chapter 1 of Kitchens monograph [1], a very clear and enjoyable mathematical introduction to topics discussed here. Diacu and Holmes [2] provide an excellent survey of symbolic dynamics applied to of celestial mechanics. Finite Markov graphs or finite automata are discussed in refs. [3, 4, 5, 6]. They belong to the category of regular languages. A good hands-on introduction to symbolic dynamics is given in ref. [12].

The binary labeling of the once-folding map periodic points was introduced by Myrberg [13] for 1-dimensional maps, and its utility to 2-dimensional maps has been emphasized in refs. [8, 12]. For 1-dimensional maps it is now customary to use the *R-L* notation of Metropolis, Stein and Stein [14, 15], indicating that the point x_n lies either to the left or to the right of the critical point in figure 10.6. The symbolic dynamics of such mappings has been extensively studied by means of the Smale horseshoes, see for example ref. [16]. Using letters rather than numerals in symbol dynamics alphabets probably reflects good taste. We prefer numerals for their computational convenience, as they speed up the implementation of conversions into the topological coordinates (δ, γ) introduced in sect. 11.4.1. The alternating binary ordering of figure 10.9 is related to the Gray codes of computer science [12].

Remark 10.2 Counting prime cycles. Duval has an efficient algorithm for generating Lyndon words (non-periodic necklaces, i.e., prime cycle itineraries).

Remark 10.3 Inflating Markov graphs. In the above examples the symbolic dynamics has been encoded by labeling links in the Markov graph. Alternatively one can encode the dynamics by labeling the nodes, as in figure 10.12, where the 4 nodes refer to 4 Markov partition regions $\{\mathcal{M}_{00}, \mathcal{M}_{01}, \mathcal{M}_{10}, \mathcal{M}_{11}\}$, and the 8 links to the 8 non-zero entries in the 2-step memory transition matrix (10.13).

fast track:
chapter 13, p. 212

Exercises

10.1. **Binary symbolic dynamics.** Verify that the shortest prime binary cycles of the unimodal repeller of figure 10.6 are $\overline{0}$, $\overline{1}$, $\overline{01}$, $\overline{001}$, $\overline{011}$, $\cdots$. Compare with table 10.1. Try to sketch them in the graph of the unimodal function $f(x)$; compare ordering of the periodic points with figure 10.9. The point is that while overlayed on each other the longer cycles look like a hopeless jumble, the cycle points are clearly and logically ordered by the alternating binary tree.

10.2. **Generating prime cycles.** Write a program that generates all binary prime cycles up to given finite length.

10.3. **A contracting baker's map.** Consider a contracting (or "dissipative") baker's defined in exercise 4.6.

The symbolic dynamics encoding of trajectories is realized via symbols 0 ($y \le 1/2$) and 1 ($y > 1/2$). Consider the observable $a(x, y) = x$. Verify that for any periodic orbit p ($\epsilon_1 \ldots \epsilon_{n_p}$), $\epsilon_i \in \{0, 1\}$

$$A_p = \frac{3}{4} \sum_{j=1}^{n_p} \delta_{j,1}.$$

10.4. **Unimodal map symbolic dynamics.** Show that the tent map point $\gamma(S^+)$ with future itinerary S^+ is given by converting the sequence of s_n's into a binary number by the algorithm (10.9). This follows by inspection from the binary tree of figure 10.9.

10.5. **Unimodal map kneading value.** Consider the 1-d quadratic map

$$f(x) = Ax(1 - x), \qquad A = 3.8. \qquad (10.23)$$

(a) (easy) Plot (10.23), and the first 4-8 (whatever looks better) iterates of the critical point $x_c = 1/2$.

(b) (hard) Draw corresponding intervals of the partition of the unit interval as levels of a Cantor set, as in the symbolic dynamics partition of figure 10.6 (b). Note, however, that some of the intervals of figure 10.6 (b) do not appear in this case - they are *pruned*.

(c) (medium) Produce ChaosBook.org quality figure 10.6 (a).

(d) (easy) Check numerically that $K = S^+(x_c)$, the itinerary or the "kneading sequence" of the critical point is

$$K = 10110111101101111010111110111110\ldots$$

The tent map point $\gamma(S^+)$ with future itinerary S^+ is given by converting the sequence of s_n's into a binary number by the algorithm (10.9),

$$w_{n+1} = \begin{cases} w_n & \text{if } s_{n+1} = 0 \\ 1 - w_n & \text{if } s_{n+1} = 1 \end{cases}, \qquad w_1 =$$

$$\gamma(S^+) = 0.w_1 w_2 w_3 \ldots = \sum_{n=1}^{\infty} w_n / 2^n.$$

(e) (medium) List the the corresponding kneading value (10.10) sequence $\kappa = \gamma(K)$ to the same number of digits as K.

(f) (hard) Plot the missing dike map, figure 10.10, in ChaosBook.org quality, with the same kneading sequence K as $f(x)$. The dike map is obtained by slicing off all $\gamma(S^+(x_0)) > \kappa$, from the complete tent map figure 10.6 (a), see (10.11).

exerKnead - 4jun2003.tex

How this kneading sequence is converted into a series of pruning rules is a dark art, relegated to sect. 13.6.

10.6. **"Golden mean" pruned map.** Consider a symmetrical tent map on the unit interval such that its highest point belongs to a 3-cycle:
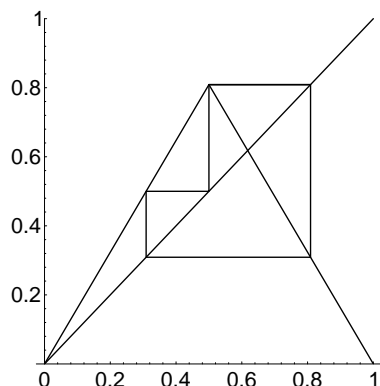
(a) Find the absolute value Λ for the slope (the two different slopes $\pm\Lambda$ just differ by a sign) where the maximum at $1/2$ is part of a period three orbit, as in the figure.

(b) Show that no orbit of this map can visit the region $x > (1 + \sqrt{5})/4$ more than once. Verify that once an orbit exceeds $x > (\sqrt{5}-1)/4$, it does not reenter the region $x < (\sqrt{5} - 1)/4$.

(c) If an orbit is in the interval $(\sqrt{5} - 1)/4 < x < 1/2$, where will it be on the next iteration?

(d) If the symbolic dynamics is such that for $x < 1/2$ we use the symbol 0 and for $x > 1/2$ we use the symbol 1, show that no periodic orbit will have the substring _00_ in it.

(e) On the second thought, is there a periodic orbit that violates the above _00_ pruning rule?

For continuation, see exercise 13.6 and exercise 17.2. See also exercise 13.7 and exercise 13.8.

10.7. **Binary 3-step transition matrix.** Construct [8×8] binary 3-step transition matrix analogous to the 2-step transition matrix (10.13). Convince yourself that the number of terms of contributing to $\mathrm{tr}\, T^n$ is independent of the memory length, and that this $[2^m \times 2^m]$ trace is well defined in the infinite memory limit $m \to \infty$.

References

[10.1] B.P. Kitchens, Symbolic dynamics: one-sided, two-sided, and countable state Markov shifts (Springer, Berlin 1998).

[10.2] F. Diacu and P. Holmes, *Celestial Encounters, The Origins of Chaos and Stability* (Princeton Univ. Press, Princeton NJ 1996).

[10.3] A. Salomaa, *Formal Languages* (Academic Press, San Diego, 1973).

[10.4] J.E. Hopcroft and J.D. Ullman, *Introduction to Automata Theory, Languages, and Computation* (Addison-Wesley, Reading MA, 1979).

[10.5] D.M. Cvetković, M. Doob and H. Sachs, *Spectra of Graphs* (Academic Press, New York, 1980).

[10.6] P. Grassberger, "On the symbolic dynamics of the one-humped map of the interval" *Z. Naturforsch. A* **43**, 671 (1988).

[10.7] P. Grassberger, R. Badii and A. Politi, *Scaling laws for invariant measures on hyperbolic and nonhyperbolic attractors*, *J. Stat. Phys.* **51**, 135 (1988).

[10.8] S. Isola and A. Politi, "Universal encoding for unimodal maps," *J. Stat. Phys.* **61**, 259 (1990).

[10.9] Y. Wang and H. Xie, "Grammatical complexity of unimodal maps with eventually periodic kneading sequences," *Nonlinearity* **7**, 1419 (1994).